

Numerical aspect of large-scale electronic state calculation for flexible device material

Takeo Hoshi · Hiroto Imachi · Akiyoshi
Kuwata · Kohsuke Kakuda · Takatoshi
Fujita · Hiroyuki Matsui

Received: date / Accepted: date

Abstract Numerical aspects of large-scale electronic state calculation are explored on flexible organic device materials. Physical theory, numerical method and real application studies are discussed in the context of application-algorithm-architecture co-design. The application studies were carried out for disordered organic thin film and polymer. Participation ratio, a measure for the spatial extension of electronic wavefunction is calculated, commonly, as a crucial physical quantity for device property. These application studies indicate the

The present research was partially supported by JST-CREST project of 'Development of an Eigen-Supercomputing Engine using a Post-Petascale Hierarchical Model', Priority Issue 7 of the post-K project and KAKENHI funds (16KT0016,17H02828). Oakforest-PACS was used through the JHPCN Project (jh170058-NAHI) and through Interdisciplinary Computational Science Program in Center for Computational Sciences, University of Tsukuba. The K computer was used in the HPCI System Research Projects (hp180079, hp180219). Several computations were carried out also on the facilities of the Supercomputer Center, the Institute for Solid State Physics, the University of Tokyo.

T. Hoshi A. Kuwata K. Kakuda
Department of Applied Mathematics and Physics, Tottori University, 4-101 Koyama-Minami, Tottori, 680-8552, Japan
Tel.: +81-857-31-5448
Fax: +81-857-31-5747
E-mail: hoshi@damp.tottori-u.ac.jp

H. Imachi
Department of Applied Mathematics and Physics, Tottori University, 4-101 Koyama-Minami, Tottori, 680-8552, Japan
Present address: Preferred Networks, Inc.

T. Fujita
Department of Theoretical and Computational Molecular Science, Institute for Molecular Science, Japan

H. Matsui
Research Center of Organic Electronics, Yamagata University, Japan

potential need of purpose-specific solvers with internal eigenpairs or mixed precision technique, which will be fruitful in (pre-)exascale supercomputers.

Keywords Large-scale electronic state calculation · generalized eigenvalue problem · organic flexible device · massively parallel supercomputer

1 Introduction

Large-scale quantum material simulation or electronic state calculation is one of the major fields in computational science with supercomputers. A central problem in this field is the generalized eigenvalue equation. Although the *de fact* standard parallel solver library is ScaLAPACK [1], these routines show severe limitations in parallel efficiency and several scalable solvers, such as ELPA [2], [3] and EigenExa [4], [5], were developed recently. Among them, ELPA was developed in the tight collaboration between numerical researchers and material researchers in Europe. [6, 3] Such a fruitful collaboration requires the co-design approach among application, algorithm and architecture, because an optimal algorithm is dependent both on problem and architecture. For example, a ELPA paper [3] discusses the benchmark of the calculation that obtains all the eigenvalues and a small fraction (10-50 %) of eigenvectors, since such calculations are typical among electronic state calculations.

The present paper reports large-scale electronic state calculations in the context of application-algorithm-architecture co-design. The target application is organic flexible device materials, and the application study contains (i) large single problem and (ii) many small problems in data scientific research. These researches lead us to a potential need for purpose-specific numerical solvers with internal eigenpair computation or mixed precision technique. We believe that the present paper is a seed of the collaboration between numerical researcher and material researcher with the next-generation or (pre-)exascale supercomputers.

The present paper is organized as follows; Physical theory and related numerical method of large-scale electronic state calculation appear in Sec. 2. Application studies appear for organic thin film in Sec. 3.1 and for organic polymer in Sec. 3.2. The potential need for purpose-specific solvers is discussed in Sec. 3.3. Section 4 is devoted to summary and future outlook.

2 Theory and numerical method

Numerical foundation of electronic state calculations is explained as the basics of the co-design approach. Details of the physical theory can be found in textbooks, such as Ref. [7].

2.1 Physical origin of matrix problem

The fundamental Schrödinger-type equation, a partial differential equation in real space \mathbf{r} , is written for an electronic wavefunction $\phi(\mathbf{r})$ as

$$\hat{H}\phi(\mathbf{r}) = \lambda\phi(\mathbf{r}) \quad (1)$$

with the Hamilton operator of

$$\hat{H} \equiv -\frac{\hbar^2}{2m}\Delta + V_{\text{eff}}(\mathbf{r}). \quad (2)$$

Here, Δ is Laplacian, m is the mass of electron and \hbar is the Planck constant, a physical constant ($\hbar \approx 1.05 \times 10^{-34}$ Js). $V_{\text{eff}}(\mathbf{r})$ is the effective potential, a scalar function. The normalization condition of

$$\int |\phi(\mathbf{r})|^2 = 1 \quad (3)$$

is imposed and stems from the fact that the sum of the weight distribution of one electron should be the unity. The function of $n(\mathbf{r}) \equiv |\phi(\mathbf{r})|^2 (\geq 0)$ is the weight distribution of the electron at the point of \mathbf{r} . The normalization condition of Eq. (3) can be expressed as

$$\int n(\mathbf{r})d\mathbf{r} = 1. \quad (4)$$

An eigenvalue of λ means the energy of an electron in the material and is called eigenenergy. The k -th eigenpair of $(\lambda_k, \phi_k(\mathbf{r}))$ is defined for $k = 1, 2, \dots, M$ in the order of $\lambda_1 \leq \lambda_2 \leq \dots \leq \lambda_M$. Each material has a specific integer of k_{HO} called highest occupied eigenenergy, and the eigenpairs for $k = 1, 2, \dots, k_{\text{HO}}$ are occupied by the electrons. A para-spin material with N_{elec} electrons, for example, gives the value of $k_{\text{HO}} = N_{\text{elec}}/2$, if N_{elec} is even. Semiconductor material has a finite energy gap between the k_{HO} -th and $(k_{\text{HO}} + 1)$ -th eigenenergies ($\lambda_{k_{\text{HO}}+1} - \lambda_{k_{\text{HO}}} > 0$).

Now we consider, as a typical case, that $\phi(\mathbf{r})$ is expressed as a linear combination of given basic functions

$$\phi(\mathbf{r}) = \sum_j^M v_j \chi_j(\mathbf{r}). \quad (5)$$

The basis functions $\{\chi_j(\mathbf{r})\}$ are normalized to be

$$\int \chi_j^*(\mathbf{r})\chi_j(\mathbf{r})d\mathbf{r} = 1. \quad (6)$$

A typical function is called atomic orbital and is localized near the position of an atomic nucleus. Since each basis function belongs to one atom, the basis index i is equivalent to the composite indices of an atom index I and an orbital

index α ($i \equiv (I, \alpha)$). The orbital index α distinguishes the basis functions that belong to the same atom but different in their shape.

A generalized eigenvalue equation appears, when Eq (5) is substituted for Eq. (1);

$$A\mathbf{v} = \lambda B\mathbf{v} \quad (7)$$

with the $M \times M$ matrices of

$$A_{ij} \equiv \int \chi_i^*(\mathbf{r}) \hat{H} \chi_j(\mathbf{r}) d\mathbf{r} \quad (8)$$

$$B_{ij} \equiv \int \chi_i^*(\mathbf{r}) \chi_j(\mathbf{r}) d\mathbf{r}. \quad (9)$$

The matrices A and B are Hermitian. The matrix B is positive definite and satisfies $B_{jj} = 1$ and $|B_{ij}| < 1 (i \neq j)$. Hereafter we consider, as among many researches, that the basis functions are real and the matrices A and B are real-symmetric. The normalization condition of Eq. (3) is reduced to

$$\mathbf{v}^T B \mathbf{v} = 1, \quad (10)$$

which is called B -normalization. The present paper will discuss matrix data generated by our simulation software ELSESES [8], [9], an electronic-state calculation software with first-principles-based modeled (tight-binding) electronic-state theory. Sparsity of the matrices of A_{ij} and B_{ij} are explained briefly. As explained in the previous subsection, the indices i and j are the composite indices of the atom indices I and J and the orbital indices α and β , respectively ($i \equiv i(I, \alpha), j \equiv j(J, \beta)$). Therefore, an element of the matrices A and B is expressed by the four indices as $A_{I\alpha;J\beta}$ and $B_{I\alpha;J\beta}$, respectively. Since a matrix element value decreases quickly and monotonically as the function of the inter-atomic distance between the I -th and J -th atoms (r_{IJ}), a cutoff distance r_{cut} can be introduced. A matrix element, $A_{I\alpha;J\beta}$ or $B_{I\alpha;J\beta}$, is ignored, if $r_{IJ} > r_{\text{cut}}$, which makes the matrices to be sparse.

2.2 Mulliken weight

This subsection introduces Mulliken weight [10], a famous discretized representation for the weight distribution of $n(\mathbf{r})$. When the quantity of $q_i^{(\text{bas})}$ is defined as

$$q_i^{(\text{bas})} \equiv \sum_j v_i B_{ij} v_j, \quad (11)$$

for $i = 1, 2, \dots, M$, it is called Mulliken weight at the i -th basis function. The normalization condition of Eq. (10) is reduced to

$$\sum_i q_i^{(\text{bas})} = 1, \quad (12)$$

which is analogous to Eq. (4).

Since the basis index of i is the composite indices of the atom index of I and the orbital index of α ($i \equiv (I, \alpha)$), the Mulliken weight at the I -th atom is defined as

$$q_I^{(\text{atm})} \equiv \sum_{\alpha} q_{I,\alpha}^{(\text{bas})} \quad (13)$$

and satisfies

$$\sum_I q_I^{(\text{atm})} = 1. \quad (14)$$

If each atom belongs to one molecule, the Mulliken weight at the P -th molecule is defined as

$$q_P^{(\text{mol})} \equiv \sum_{I \in P} q_I^{(\text{atm})}, \quad (15)$$

where $\sum_{I \in P}$ is the summation among the atoms that belong to the P -th molecule. The sum is the unity;

$$\sum_P q_P^{(\text{mol})} = 1. \quad (16)$$

In this paper, we will use the definition of $\mathbf{q}^{(\text{bas})} \equiv (q_1^{(\text{bas})}, q_2^{(\text{bas})}, \dots, q_{\mu}^{(\text{bas})})^T$ and $\mathbf{q}^{(\text{mol})} \equiv (q_1^{(\text{mol})}, q_2^{(\text{mol})}, \dots, q_{\mu}^{(\text{mol})})^T$, where μ is the number of the molecules in the system.

2.3 Participation ratio

This subsection introduces participation ratio (PR), as a measure of the spatial extension of wavefunctions $\phi(\mathbf{r})$ or how the wavefunction spreads in real space [11], [12], [13], [14]. Since the spatial extension of wavefunction governs the electrical conductivity, PR was used with large-scale electronic state calculations, such as a research on the anomalous electrical conductivity in quasi crystals [15].

In the continuum representation, PR is defined for a wavefunction $\phi(\mathbf{r})$ as

$$P^{(\text{cnt})^{(4)}}(\phi) \equiv \left(\int |\phi(\mathbf{r})|^4 d\mathbf{r} \right)^{-1}. \quad (17)$$

under the L^2 -normalization of Eq. (3). For example, suppose D is a closed area whose volume is Ω and ϕ is constant in D as

$$\phi(\mathbf{r}) = \begin{cases} \frac{1}{\sqrt{\Omega}} & (\mathbf{r} \in D) \\ 0 & (\text{otherwise}). \end{cases} \quad (18)$$

Then the PR of ϕ gives the volume of the non-zero region of ϕ

$$P^{(\text{cnt})(4)}(\phi) = \left(\frac{1}{\Omega^2} \int_D d\mathbf{r} \right)^{-1} = \Omega. \quad (19)$$

The above definition of PR can be expressed also by the weight distribution of $n(\mathbf{r})$ as

$$P^{(\text{cnt})(2)}(n) \equiv \left(\int |n(\mathbf{r})|^2 d\mathbf{r} \right)^{-1} \quad (20)$$

under the normalization of Eq. (4).

PR for the eigenvector of $\mathbf{v} \equiv (v_1, v_2, \dots, v_M)^T$ in Eq. (7) can be also defined in a similar manner. The definition in the present paper is

$$P^{(4)}(\mathbf{v}) \equiv (\|\mathbf{v}\|_4)^{-1} \quad (21)$$

under the B -normalization constraint of Eq. (10). For the discretized representation, PR indicates a measure of the number of non-zero elements, namely, how broadly the elements exist on the indices. For example, the case of $B = I$ and

$$\mathbf{v} \equiv \left(\frac{1}{\sqrt{3}}, \frac{1}{\sqrt{3}}, \frac{1}{\sqrt{3}}, 0, 0, \dots, 0 \right)^T, \quad (22)$$

the PR is

$$P^{(4)} = \left\{ \sum_j |v_j|^4 \right\}^{-1} = \left\{ 3 \left(\frac{1}{\sqrt{3}} \right)^4 \right\}^{-1} = 3. \quad (23)$$

Another definition is the one for the Mulliken weight on basis function as

$$P^{(2)}(\mathbf{q}^{(\text{bas})}) \equiv (\|\mathbf{q}^{(\text{bas})}\|_2)^{-1} \quad (24)$$

or the one for the Mulliken weight on molecules as

$$P^{(2)}(\mathbf{q}^{(\text{mol})}) \equiv (\|\mathbf{q}^{(\text{mol})}\|_2)^{-1}. \quad (25)$$

The quantity of Eq.(25) is called ‘molecular PR’ in this paper and will appear later in this paper.

2.4 Sparsity of matrix data

According to the physical origin, the sparsity in matrix data of A and B is determined by the atomic structure of the simulated system. If a system contains independent (non-interacting) molecules, for example, the matrices of A and B are block diagonal and, each block stems from a molecule. The sparsity of the matrices is crucial for the efficiency of sparse-matrix solvers. A matrix data library of ‘ELSES matrix library’ [16] was constructed, so as to enhance the collaboration between material and numerical researchers. The sparsity is different among the matrix data, as seen in Fig. 3 of Ref. [17], for example. Two examples are explained; The matrix data of ‘APF4686’ stems from an organic polymer system, poly-(9,9 dioctyl-fluorene), in a disordered structure with 2076 atoms [9], [18]. The matrix size of is $M = 4686$ and the number of non-zero elements is $N_{\text{NZ}} = 53950$. The ratio of non-zero elements is $\gamma \equiv N_{\text{NZ}}/M^2 \approx 0.0025$. On the other hand, the matrix data of ‘AUNW9180’ stems from a disordered multishell gold nanowires with 1020 atoms [19]. The matrix size of is $M = 9180$ and the number of non-zero elements is $N_{\text{NZ}} = 1783313$. The ratio of non-zero elements is $\gamma \equiv N_{\text{NZ}}/M^2 \approx 0.021$. It is noteworthy that ELSES matrix library has several features for the convenience of numerical researchers; (i) The matrix data files are recorded in the Matrix-Market format. [20] (ii) Eigenvalues and PR values are stored as files, as well as the matrix data.

3 Application to organic device materials

The present section is devoted to application study for large-scale electronic state calculations of organic semiconductor materials. Organic semiconductor materials form the foundation of flexible devices such as flexible displays [21], flexible solar cells [22], and human-friendly wearable electronics [23]. Since complicated disordered structure is crucial for device properties such as device performance or device lifetime, large-scale simulations in 10-100 nm scales are required.

The present paper focuses on p-type semiconductor, in which the electrical current stems from a small number of wavefunctions that has the internal eigenenergies λ_k near the highest occupied one λ_{HO} ($\lambda_k \leq \lambda_{\text{HO}}$). Therefore, one should calculate only these internal eigenpairs. Such wavefunctions lie for example, on benzene ring regions and are called π electrons.

The device property is related to the spatial extension of the π electrons which is measured by PR. A fundamental issue in the industrial viewpoint is a conflicting demand on opt-electronic devices; An extended wavefunction is preferable for conduction property, since an extended wavefunction can induce the electrical current easily. A localized wavefunction, by contrast, is preferable for optical property, since a localized wavefunction can strongly interact with light. The above conflicting demand should be a foundation of material design. Wavefunctions in disordered structures are localized, while wavefunc-

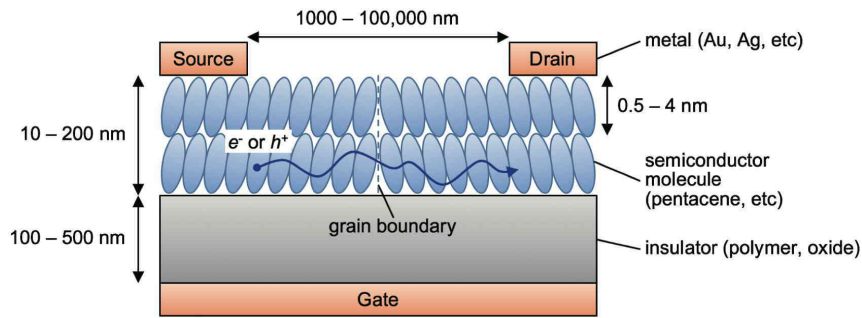


Fig. 1 Schematic structure and typical scales of organic field-effect transistors. The electrical current is depicted as an arrow squiggle.

tions in ideal crystalline (periodic) structures are extended throughout the whole system.

The generalized eigenvalue problem was solved by the mini-application of EigenKernel [24], [25], [26]. EigenKernel is a middleware for the various solvers in ScaLAPACK, ELPA, and EigenExa and their hybrids. Although we have developed a massively parallel electronic state calculation method without eigenvalue problem [8], [9], [27], we still need eigenvalue solver, so as to obtain eigenpairs in the discussion of electronic property.

3.1 Large-scale calculation of thin film organic material

The present subsection is devoted to thin film or two-dimensional condensed organic semiconductor molecules in disordered structures, which is a prototypical system of organic field-effect transistors (OFETs) shown schematically in Fig. 1. OFETs consist of four layers: a gate electrode layer, an insulating layer, an organic semiconductor layer, and a source/drain electrode layer, typical scales of which are shown in Fig. 1. The details of Fig. 1 is explained in textbooks, like Ref. [28]. In the OFETs, the electrical current flows on several atomic semiconductor layers on the interface region between the polycrystalline semiconductor and amorphous insulator layers. So we focus on a thin film system with disordered structures. The present calculated system is a thin film of pentacene molecules ($C_{22}H_{14}$). Pentacene is one of the most famous organic semiconductors. The present study is motivated by an experimental data of electron spin resonance (ESR) experiment for pentacene OFETs [29, 30]. The analysis of hyperfine interaction between hole carriers and protons in pentacene thin film in ESR spectra gives a molecular PR defined in Eq.(25) [29]. The molecular PR is denoted as P hereafter. The experimental data indicates the appearance of ‘semi-localized’ wavefunction that is extended among a few tens of molecules ($P = O(10)$). Such semi-locality is crucial for the device performance.

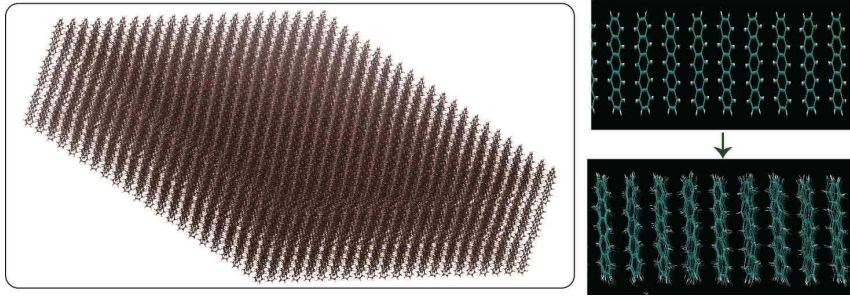


Fig. 2 Preparation of disordered pentacene thin film sample. (a) The initial structure of a three-layered sample in the crystalline geometry. (b) The result of finite-temperature simulation.

An important industrial issue is to control the disorder of the atomic structure without an increase of the fabrication cost. If the atomic structure is fairly disordered, electronic wavefunction will be localized and the material will show a poor device property. The above situation gives a strong need of electronic state calculation for a large-scale disordered thin film.

The calculated system is a thin-film (single molecular layer) system with an artificial two-dimensional periodic simulation cell. The simulation cell contains $N_{\text{mol}}=1800$ molecules, and the matrix size of the generalized eigenvalue problem is $M = 183600$. Thousands of molecules are required in the simulation cell, so as to observe a semi-localized state extended among tens of molecules ($N_{\text{mol}} \gg O(10)$).

The initial atomic structure of the disordered thin film sample was generated in classical molecular dynamics simulations by GROMACS [31], [32] with the generalized AMBER force field (GAFF) parameter set [33]. The software and parameter set are standard for organic materials. The sample was prepared in the following stages; (I) A layered structure of pentacene in the crystalline geometry was prepared with three layers, shown in Fig. 2(a). (II) Finite temperature simulation with 300 K for 1 ns was carried out, so as to generate a high-temperature disordered structure, as shown in Fig. 2(b). In the simulation, only the middle layer Fig. 2(a) was set to be mobile, and the upper and lower layers were set to be fixed, so as to impose the boundary condition on the middle layer. It is noteworthy that such a long-time (nano-second) dynamics can not be carried out by quantum simulation, owing to huge CPU time and we used the classical simulation. Classical simulations, however, do not treat electronic wavefunction, and the electronic state calculation is required for the disordered structure, so as to obtain wavefunctions.

Figure 3 shows a typical wavefunction with the molecular PR of $P \approx 35$, which agrees with the experimental observation of semi-localized wavefunction ($P = O(10)$). We should say, however, that the present simulation is the one for an isolated thin film system of pentacene layer and ignores the affects the neighboring layers, whereas the experimental result [29,30] indicates the importance of the neighboring insulator layer shown in Fig. 1. Now the cal-

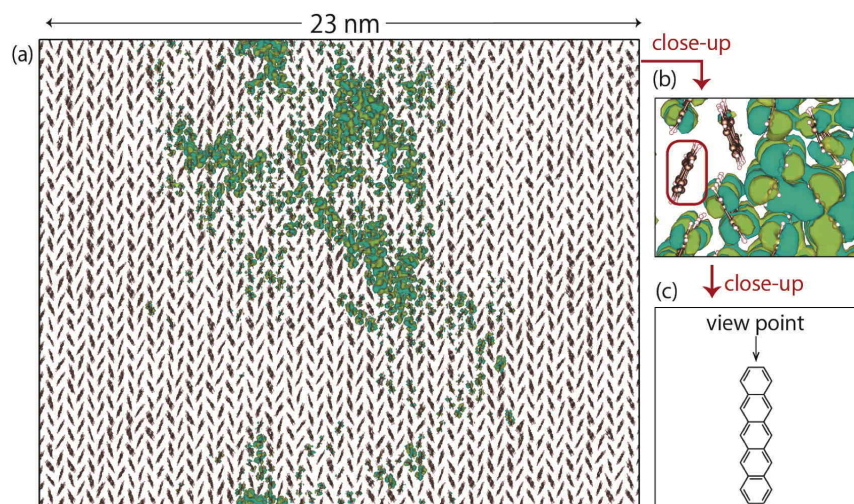


Fig. 3 Example of semi-localized wavefunction that appears on a pentacene thin-film system. The wavefunction $\phi(\mathbf{r})$ has the eigenenergy of $\lambda \approx -0.15\text{eV}$, where the energy origin ($\lambda \equiv 0$) is set to be the eigenenergy of the highest occupied wavefunction. The wavefunction of $\phi(\mathbf{r})$ is depicted as two iso-surfaces in the opposite signs ($\phi(\mathbf{r}) = \pm C$, where C is a positive constant). The two surfaces are painted by different colors. (a) The whole region of the periodic simulation cell. (b) A close-up of (a). (c) A picture of a single pentacene molecule with the view point of (b).

culations are on going for the interface system including pentacene layer and insulator layers.

3.2 Data scientific research of organic polymers

This subsection gives a data scientific research with capacity computation, or simultaneous computation of many middle-size problems. The purpose of the research is how to characterize the disordered structure in the context of device property. In general, the spatial extension of wavefunction plays a crucial role on device property and is rigorously measured by PR for each wavefunction. Therefore a set of PR values among wavefunctions in a sample can be a candidate of the measure of the disorder for the sample. In other words, the set of PR values can be a descriptor that characterizes the sample.

The present paper focuses on a research on poly-(phenylene-ethynylene) (PPE) [34], a typical conducting polymer. The paper measures the device property or the mobility for isolated polymers and found the importance of structural disorder. The first stage of theoretical research on disordered polymers is to define the descriptor of disordered polymers. The present paper proposes that the set of PR values can give a descriptor for a disordered sample.

Figure 4 shows a classification problem among $N_{\text{sample}} = 200$ disordered PPE polymer samples by the K-means clustering method, a typical classification algorithm. The structure of PPE polymers consists of 240 atoms, and a part is drawn in the inset of Fig. 4. A polymer sample consists of 20 benzene rings. The structural disorder was introduced in the relative rotation angles between adjacent benzene rings shown in θ in Fig. 4. The angles were set from the normal distribution with standard deviation of 20 or 60 degree. The samples were generated 100 times for each class (total $N_{\text{sample}} = 200$ samples). After the rotations, small fluctuations taken from the normal distribution with standard deviation of 0.01 Å were given to all the coordinates of all atoms to remove degeneracy. For each sample ($i = 1, \dots, N_{\text{sample}}$), the generalized eigenvalue problem of

$$H^{(i)}\mathbf{v}_j^{(i)} = \lambda_j^{(i)}S^{(i)}\mathbf{v}_j^{(i)} \quad (j = 1, \dots, M). \quad (26)$$

was solved numerically with the matrix size of $M = 714$. Here, the list of PR value of all the eigenvectors

$$\mathbf{d}^{(i)} := (P^{(4)}(\mathbf{v}_1^{(i)}), \dots, P^{(4)}(\mathbf{v}_M^{(i)}))^T \quad (27)$$

was used as the descriptor vector for the i -th sample.

The classification in the K-means clustering algorithm was carried out with the descriptor vectors of $\{\mathbf{d}^{(i)}\}_{i=1, \dots, M}$. The number of clusters was two. The classification result is shown in Fig. 4. Each sample is plotted on the plane by two statistical quantities with markers corresponding to the cluster labels given by the K-means algorithm. As a result, the two clusters perfectly matched to the structure classes. Namely, all the samples with adjacent rotation angles in standard deviation of 20 degree are clustered into one group, and all the samples with adjacent rotation angles in standard deviation of 60 degree are clustered into the other group. We should note the generality of PR as descriptor, since PR is calculated uniquely for any material without any preknowledge. The present result implies that the PR of wavefunctions can be an important quantity that bridges between disordered structure and device property. A more extensive study with principal component analysis is on going [35] and will be reported elsewhere.

3.3 Potential needs of purpose-specific solvers

Potential needs of purpose-specific solvers appear from the two application studies in the previous subsections and are discussed here for possible future collaboration between numerical and material researchers.

The first need is the one for the solver of internal eigenpairs, like z-PARES[36],[37], FEAST[38],[39], the filtering method [40], k-ep [17], [41], because we would like to calculate only internal eigenpairs with the eigenenergies λ_k near the highest occupied one λ_{HO} ($\lambda_k \leq \lambda_{\text{HO}}$). Internal eigenpair solvers are desirable both for a solution of large problems, or a faster solution of middle-size problems.

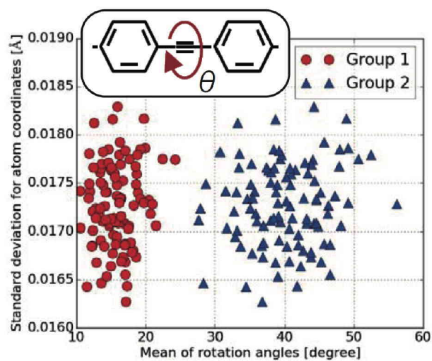


Fig. 4 K-means clustering of polymer structures by their eigenvector participation ratios. Each structure is plotted by two statistical quantities. The x-axis is the mean of the rotation angles between adjacent benzene rings. The y-axis is the resulting standard deviation of the small fluctuation to the coordinates. Two markers, red circle and blue triangle, correspond to the two clusters labeled by the K-means algorithm.

Application researchers, however, find sometimes the difficulty in choosing a solver, since the performance can be dependent on problem and machine. For example, the performance is dependent not only the matrix size M but also the sparsity, when one uses a sparse-matrix solver. A possible remedy for the difficulty is to develop a ‘middleware’ that provides a universal interface for various solver routines, like EigenKernel.

The second need is the possible acceleration by mixed precision technique or any other methods with lower accuracy. The purpose of the eigenvalue problems in the present section is to calculate PR, not eigenvector itself. Since the discussion for disordered materials requires statistical analysis among many samples, numerical error ε_{num} is acceptable, if it is less than or equal to the statistical error ε_{sta} ($\varepsilon_{\text{num}} \leq \varepsilon_{\text{sta}}$). Consequently, the authors speculate that a solver with lower accuracy will be fruitful in the present purpose. Nowadays, the architectures in the next-generation tends to be designed to give a good performance for single- or half-precision calculation, owing to the strong need in machine learning. Therefore, the use of single- or half-precision calculation is consistent to the current design trend of architecture.

4 Summary and future outlook

The present paper discusses the generalized eigenvalue problem in large-scale electronic state calculation for flexible organic device materials. The application studies were carried out for disordered organic thin film and polymer. The calculation of participation ratio, the L^4 norm of the eigenvectors, is focused on, since it is a measure of the spatial extension of electronic wavefunctions and governs the device property. The present application research indicates the potential need of purpose-specific solvers with internal eigenpairs or mixed pre-

cision technique. The purpose-specific solvers will be fruitful in (pre-)exascale supercomputers, as an application-algorithm-architecture co-design.

Acknowledgement

The authors thank to Tomofumi Tada (Tokyo institute of Technology) and Jun Terao (University of Tokyo) for fruitful discussion on organic polymer.

References

1. ScaLAPACK: <http://www.netlib.org/scalapack/>
2. ELPA: <http://elpa.mpcdf.mpg.de/>
3. Marek, A., Blum, V., Johanni, R., Havu, V., Lang, B., Auckenthaler, T., Heinecke, A., Bungartz, H. J. and Lederer, H., 'The ELPA Library – Scalable Parallel Eigenvalue Solutions for Electronic Structure Theory and Computational Science', *J. Phys. Condens. Matter* **26** (2014) 213201.
4. EigenExa: <http://www.r-ccs.riken.jp/labs/lpnctr/en/projects/eigenexa/>
5. Imamura, T., Hirota, Y., Fukaya, T., Yamada, S., and Machida, M. 'EigenExa: high performance dense eigensolver, present and future', 8th International Workshop on Parallel Matrix Algorithms and Applications (PMAA14), Lugano, Switzerland, 2014.
6. Blum, V., Gehrke, R., Hanke, F., Havu, P., Havu, V., Ren, X., Reuter, K. and Scheffler, M.: Ab initio molecular simulations with numeric atom-centered orbitals, *Computer Physics Communications* **180** (2009) 2175-2196; <https://aimsclub.fhi-berlin.mpg.de/>
7. Martin, R. M., 'Electronic Structure - Basic Theory and Practical Methods', Cambridge University Press (2004).
8. ELSESES: <http://www.elses.jp>
9. Hoshi, T., Yamamoto, S., Fujiwara, T., Sogabe, T. and Zhang, S.-L.: An order- N electronic structure theory with generalized eigenvalue equations and its application to a ten-million-atom system, *J. Phys. Condens. Matter* **24** (2012) 165502.
10. Mulliken, R. S. 'Electronic Population Analysis on LCAO-MO Molecular Wave Functions. I', *J. Chem. Phys.* **23**, (1955) 1833-1840.
11. Bell, R. J., and Dean, P., 'Atomic vibrations in vitreous silica', *Disc. Faraday Soc.* **50**, (1970) 55-61.
12. Bell, R. J., 'The dynamics of disordered lattices', *Rep. Prog. Phys.* **35** (1972) 1315.
13. Thouless, D. J., 'Electron in disordered systems and the theory of localization', *Phys. Rep.* **13** (1974) 93-142.
14. Wegner, F., 'Inverse Participation Ratio in $2 + \epsilon$ Dimensions', *Z. Physik B* **36** (1980) 209-214.
15. Fujiwara, T., Mitsui, T., and Yamamoto, S., 'Scaling properties of wave functions and transport coefficients in quasicrystals', *Phys. Rev. B* **53** (1996) R2910-R2913.
16. ELSESES matrix library: <http://www.elses.jp/matrix/>
17. Dongjin Lee, Takeo Hoshi, Tomohiro Sogabe, Yuto Miyatake, Shao-Liang Zhang, 'Solution of the k -th eigenvalue problem in large-scale electronic structure calculations', *J. Comp. Phys.* **371** (2018) 618-632.
18. Hoshi, T., Yamazaki, K., Akiyama, Y., 'Novel linear algebraic theory and one-hundred-million-atom electronic structure calculation on the K computer', *JPS Conf. Proc.* **1** (2014) 016004/1-4.
19. Hoshi, T., and Fujiwara, T., 'Domain boundary formation in helical multishell gold nanowires', *J. Phys.: Condens. Matter* **21** (2009), 272201/1-7.
20. Matrix Market: <http://math.nist.gov/MatrixMarket/index.html>
21. Gelinck, G. H., Huitema, H. E., van Veenendaal, E., Cantatore, E., Schrijnemakers, L., van der Putten, J. B., Geuns, T. C., Beenhakkers, M., Giesbers, J. B., Huisman, B. H., Meijer, E. J., Benito, E. M., Touwslager, F. J., Marsman, A. W., van Rens, B. J., de Leeuw, D. M., 'Flexible active-matrix displays and shift registers based on solution-processed organic transistors', *Nat. Mater.* **3** (2004) 106-110.

22. Xu, X., Fukuda, K., Karki, A., Park, S., Kimura, H., Jinno, H., Watanabe, N., Yamamoto, S., Shimomura, S., Kitazawa, D., Yokota, T., Umez, S., Nguyen, T-Q., and Someya, T., 'Thermally stable, highly efficient, ultraflexible organic photovoltaics', *PNAS* 115 (2018) 4589-4594.
23. Sekitani, T., and Someya, T., 'Human-friendly organic integrated circuits', *Mater. Today* 14 (2011) 398-407.
24. Imachi, H., Hoshi, T., 'Hybrid numerical solvers for massively parallel eigenvalue computation and their benchmark with electronic structure calculations', *J. Inf. Process.* 24 (2016) 164-172.
25. EigenKernel: <https://github.com/eigenkernel/>
26. Kazuyuki Tanaka, Hiroto Imachi, Tomoya Fukumoto, Takeshi Fukaya, Yusaku Yamamoto, Takeo Hoshi, 'EigenKernel - A middleware for parallel generalized eigenvalue solvers to attain high scalability and usability', Preprint: <http://arxiv.org/abs/1806.00741>
27. Hoshi, T., Imachi, H., Kumahata, K., Terai, M., Miyamoto, K., Minami, K., and Shoji F.: Extremely scalable algorithm for 10^8 -atom quantum material simulation on the full system of the K computer, Proceeding of 7th Workshop on Latest Advances in Scalable Algorithms for Large-Scale Systems (ScalA), held in conjunction with SC16: The International Conference for High Performance Computing, Networking, Storage and Analysis Salt Lake City, Utah November, 13-18 (2016) 33-40.
28. Bao, Z., Locklin, J., 'Organic Field-Effect Transistors', CRC Press (2007)
29. Matsui, H., Mishchenko, A. S., and Hasegawa, T., Distribution of localized states from fine analysis of electron spin resonance spectra in organic transistors, *Phys. Rev. Lett.* 104, (2010) 056602/1-4.
30. Matsui, H., Mishchenko A. S. and Hasegawa, T., Origin of shallow traps in organic transistors: dipole disorder at the semiconductor/insulator interface, The 68-th Annual Meeting of the Physical Society of Japan, 27pXP-4, Hiroshima University, 26-29., Mar. (2013)
31. GROMACS: <http://www.gromacs.org/>
32. Berendsen, H. J. C., van der Spoel, D., van Drunen, R., GROMACS: A message-passing parallel molecular dynamics implementation, *Comp. Phys. Comm.* 91 (1995) 43-56.
33. Wang, J., Wolf, R. M., Caldwell, J. W., Kollmann, P. A., Case, D. A., Development and Testing of a General Amber Force Field, *Comput. Chem.* 25 (2004) 1157-1174.
34. J. Terao, A. Wadahama, A. Matono, T. Tada, S. Watanabe, S. Seki, T. Fujihara, and Y. Tsuji, 'Design principle for increasing charge mobility of π -conjugated polymers using regularly localized molecular orbitals', *Nat. Commun.* 4 (2013) 1691.
35. T. Hoshi, H. Imachi, K. Oohira, Y. Abe, and K. Hukushima, 'Principal component analysis with electronic wavefunctions for exploration of organic polymer device materials', International Meeting on High-Dimensional Data-Driven Science (HD³-2017), Kyoto, Japan, 10-13, Sep. 2017.
36. T. Sakurai, H. Sugiura, A projection method for generalized eigenvalue problems using numerical integration, *J. Comput. Appl. Math.* 159(1) (2003) 119-128.
37. z-PARES: <http://zpare.cs.tsukuba.ac.jp/>
38. E. Polizzi, Density-matrix-based algorithm for solving eigenvalue problems, *Phys. Rev. B* 79 (2009) 115112/1-6.
39. FEAST: <http://www.feast-solver.org/>
40. R. Li, Y. Xi, E. Vecharynski, C. Yang, Y. Saad, A thick-restart Lanczos algorithm with polynomial filtering for Hermitian eigenvalue problems, *SIAM J. Sci. Comput.* 38(4) (2016) A2512-A2534.
41. k-ep: <https://github.com/lee-djl/k-ep>